Invaded cluster algorithm for critical properties of periodic and aperiodic planar Ising models

2000 J. Phys. A: Math. Gen. 33 3097

(http://iopscience.iop.org/0305-4470/33/16/304)

J. Phys. A: Math. Gen. **33** (2000) 3097–3109. Printed in the UK PII: S0305-4470(00)08626-1

Invaded cluster algorithm for critical properties of periodic and aperiodic planar Ising models

Oliver Redner and Michael Baake

Institut für Theoretische Physik, Universität Tübingen, Auf der Morgenstelle 14, D-72076 Tübingen, Germany

Received 11 October 1999

Abstract. We demonstrate that the invaded cluster algorithm, introduced by Machta *et al* (1995 *Phys. Rev. Lett.* **75** 2792–5), is a fast and reliable tool for determining the critical temperature and the magnetic critical exponent of periodic and aperiodic ferromagnetic Ising models in two dimensions. The algorithm is shown to reproduce the known values of the critical temperature on various periodic and quasiperiodic graphs with an accuracy of more than three significant digits, but only modest computational effort. On two quasiperiodic graphs which were not investigated in this respect before, the 12-fold symmetric square–triangle tiling and the 10-fold symmetric Tübingen triangle tiling, we determine the critical temperature. Furthermore, a generalization of the algorithm to non-identical coupling strengths is presented and applied to a class of Ising models on the Labyrinth tiling. For generic cases in which the heuristic Harris–Luck criterion predicts deviations from the Onsager universality class, we find a magnetic critical exponent different from the Onsager value. But notable exceptions to the criterion are found which consist not only of the exactly solvable cases, in agreement with a recent exact result, but also of the self-dual ones and maybe more.

1. Introduction

Explicit exact solutions for the thermodynamic behaviour of (ferromagnetic) Ising models are available, or expected to exist, only in one dimension and for a few models in two dimensions. For more complex cases, and in higher dimensions, one has to rely on approximate techniques or simulations. As one is usually interested in the expectation value of certain observables such as the magnetization and the susceptibility at a given temperature, Monte Carlo algorithms sampling the canonical ensemble are often the numerical methods of choice.

The limiting factor in investigating the critical behaviour of spin systems with algorithms of this kind is the critical slowing at the phase transition point. The time needed to sample statistically independent system configurations diverges with the system size according to a power law. The algorithms being most efficient in this respect are the so-called cluster algorithms, the first of which was introduced by Swendsen and Wang in 1987 [34]. A single-cluster version, which shows less critical slowing in three and more dimensions, was proposed by Wolff two years later [36]. Series expansions are also suitable for studying the critical behaviour of periodic models, but they do not lead to satisfactory results for aperiodic ones [30].

Estimating the critical temperature of the infinite system with Monte Carlo algorithms is usually done using the Binder cumulant method [10]. (For example, this was used in the first paper on the universality class for quasiperiodic graphs [9] which will also play an important role in this paper.) For a number of finite system sizes and several temperature values taken from

0305-4470/00/163097+13$30.00

some interval containing the critical temperature, the fourth cumulant of the magnetization is measured. This cumulant is zero for infinite temperature, $\frac{2}{3}$ for zero temperature, and depends on the system size for all other temperature values; only at the critical temperature do the curves for different system sizes intersect. This admits rather reliable determination of the location of the critical point. However, because the system has to be simulated at several temperature values, this procedure is very time-consuming, and a rough knowledge of the location of the critical temperature is required beforehand. So, independent methods are certainly useful.

In 1995, Machta *et al* [24] developed a self-organized version of the Swendsen–Wang algorithm which they dubbed the invaded cluster (IC) algorithm. It is not only able to locate the critical temperature without prior knowledge and without any temperature sweeps being necessary, but also seems to show even less critical slowing than the Wolff algorithm [26]. The algorithm was shown to reproduce three significant digits of the known values of the critical temperature on the square and simple cubic lattice Ising models with modest computational effort [24, 25]. The ensemble that is sampled, however, is not the canonical one, and not much is known about it rigorously. In the thermodynamic limit, it is expected to be equivalent to the latter, but nothing helpful is known about the finite-size scaling. Also, the thermal exponent and equivalent quantities, such as ν and α, are not easily measured with the IC algorithm [14, 26].

This lack of theoretical knowledge is responsible for the fact that, so far, the best accuracy in measuring the critical temperature is still an order of magnitude lower than with other cluster algorithms [12]. Nevertheless, at this accuracy, the IC algorithm is substantially faster. This is mainly due to the fact that the temperature need not be varied. In addition, the autocorrelation times are, by a factor of four or more, smaller than those of the Wolff algorithm [25]. (If one is also interested in observables on sub-systems this is not true, but the autocorrelation times are still comparable with those of the Wolff algorithm, see [26].) As a rule of thumb, one can expect the IC algorithm to be at least a factor of five faster. Therefore, it is a good choice for obtaining a good estimate of the critical temperature with modest computational effort. In addition, one of the two independent critical exponents, the magnetic exponent y_h, can be measured easily.

Those quantities are of particular interest for Ising models on quasiperiodic tilings, a class of graphs being used as models for the structure of quasicrystals; compare [2, 15] and references therein. As these graphs are very homogeneous, the influence of the quasiperiodicity on the critical temperature is expected to be small and its rough location should be governed by the first mean coordination number, see [4] and references therein. The critical exponents are expected to be the same as their periodic counterparts unless the degree of disorder is bigger than a 'critical' value. This is the result of the heuristic criterion by Luck [22] who generalized the well-known Harris criterion for random disorder [16] to aperiodic structures. This criterion, now called the Harris–Luck criterion, was recently proved for certain kinds of one-dimensional disorder [17, 20] and corroborated by approximate methods for two-dimensional substitution systems [18, 19]. But in two or more dimensions, the validity has not yet been systematically confirmed by simulations.

The IC algorithm has so far only been tested on the square and the simple cubic lattice—both with success [12, 24–26]. Before its results for more complex situations can be trusted, however, it should be tested on other graphs for which the critical temperature is known. This will be done in section 2 for a number of periodic and quasiperiodic graphs. Then, as a first application, the critical temperature of the Ising model on two quasiperiodic tilings, a 12-fold symmetric square–triangle tiling [5] and the 10-fold symmetric Tübingen triangle tiling [6], will be determined. In section 3, we will present a generalization of the IC algorithm to models with arbitrary coupling strengths. Results of simulations on different realizations of the Labyrinth tiling [32] with this generalized algorithm will be described in section 4. Section 5 will give a summary and discussion.

2. The critical temperature of models with identical couplings

We consider the field-free Ising model defined by a spin $\sigma_i = \pm 1$ on each vertex i of some graph and a ferromagnetic bond $\langle i, j \rangle$ of coupling strength $J_{ij} > 0$ between each pair of neighbouring spins. The internal energy is $\mathcal{H}(\boldsymbol{\sigma}) = -\sum_{\langle i,j \rangle} J_{ij}\sigma_i\sigma_j$ where the sum is over all bonds. In this section, we restrict ourselves to identical couplings $J_{ij} \equiv 1$.

For the Ising model with this restriction, the critical temperature is known exactly on a number of periodic graphs, see [35] for a survey. In the case of two quasiperiodic tilings, the Penrose tiling [28] and the octagonal Ammann–Beenker tiling [1, 8], there exist Monte Carlo estimates [21, 27, 33] and high-precision numerical values from a recent analysis of large periodic approximants using Kac–Ward determinants [31]. With those values, the critical temperature on the corresponding dual tilings is also known, through the exact relationship [35]

$$\sinh(2\beta_c)\sinh(2\beta_c^*) = 1 \tag{1}$$

where β_c and β_c^* are the inverse critical temperatures on a graph and its dual. All this offers a number of graphs on which the IC algorithm can be tested thoroughly.

With the IC algorithm, a given configuration of a (finite-sized) system is updated in two steps. First, bonds between aligned spins (*satisfied* bonds) are selected in random order until one connected component (*cluster*) wraps around the system in at least one dimension (periodic boundary conditions are assumed) or all satisfied bonds have been selected. Then, each cluster (including each isolated spin) is flipped with probability $\frac{1}{2}$. The fraction of selected to satisfied bonds, f, gives an estimate β_{est} of the inverse critical temperature via [24]

$$f = 1 - \mathrm{e}^{-2\beta_{est}}. \tag{2}$$

This is reasonable, as the expectation value of f in the canonical ensemble is just the probability $p = 1 - \mathrm{e}^{-2\beta}$ to select a bond in the Swendsen–Wang algorithm.

For each periodic graph depicted in figure 1, we used the IC algorithm to simulate the Ising model at 13 different linear system sizes L between 16 and 288. For the quasiperiodic tilings, shown in figure 2, we had to restrict ourselves to the periodic approximants available. With each size, 10 bunches of 5000 update steps each were taken. This took approximately 2.3×10^{-6} s per bond on a 266 MHz Pentium II processor which amounts to roughly one day for all sizes of one graph. The first bunch was used for equilibration and then discarded. For each one of the remaining, the averages of the quantities of interest were computed and those numbers treated as an independent sample.

In contrast to the previous IC studies [12,24–26], in which the average of f was determined and β_{est} inferred in the end using (2), we computed β_{est} in each step. This leads to the same results after finite-size scaling, as shown in [29]. Figure 3 shows the results for the estimates of the inverse critical temperature on the hexagon packing as a typical example. The picture is qualitatively the same for all graphs considered: details can be found in [29]. Due to certain bottlenecks occurring in the cluster growth process [25], the mean value of β_{est} is always greater than the median. But both are expected to approach the same value β_c in the thermodynamic limit $L \to \infty$. From the data it is obvious that both curves are inclined towards each other. This gives rise to the following recipe for estimating β_c and its error. We compute linear fits to both the mean and median values independently using the data points corresponding to some of the largest system sizes. Then we take the mean of both β_c-axis intercepts as an estimate for β_c and half their separation as its error.

There is no *a priori* justification for this recipe besides the numerical evidence that β_c lies in between both points. The results shown in table 1 agree with the known values to within more than three significant digits. This indicates that the way β_c is estimated is reasonable and that we considerably overestimate the error. For the Penrose and the Ammann–Beenker tiling,

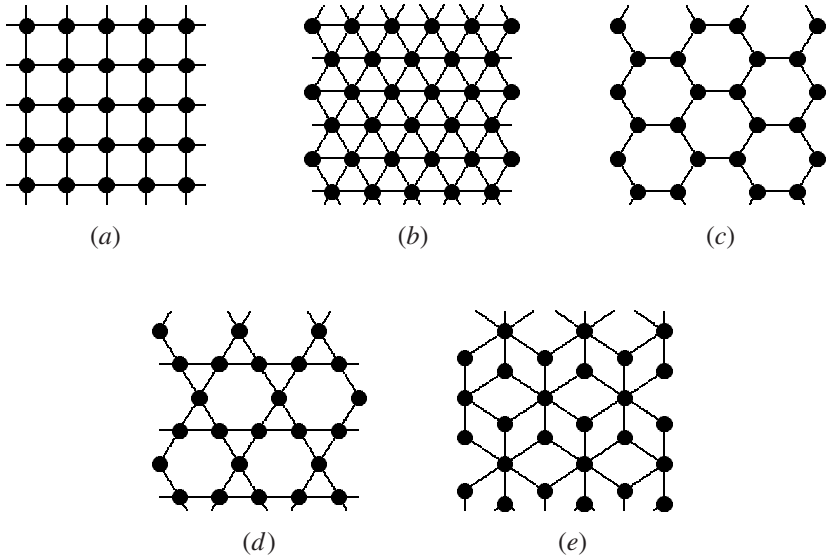

Figure 1. Parts of the periodic graphs considered here: (*a*) square lattice, (*b*) triangular lattice, (*c*) hexagon packing, (*d*) Kagomé graph and (*e*) diced graph.

Table 1. IC estimates of the inverse critical temperature for various graphs. Note that the errors given are very conservative upper bounds. Exact and other numerical values are given for comparison where available. The exact values are taken from [35], the best numerical ones from [31]. The values for the dual tilings marked with * were inferred using the exact relation (1).

	β_c			(Mean) coordination
Graph	Exact/best	IC estimate	Other values	number
Square lattice	0.440 686 8 . . .	0.440 5(4)		4
Triangular lattice	0.274 653 1 . . .	0.274 7(5)		6
Hexagon packing	0.658 478 9 . . .	0.658 4(11)		3
Kagomé graph	0.466 566 0 . . .	0.466 5(8)		4
Diced graph	0.415 721 5 . . .	0.415 7(7)		4
Penrose tiling	0.417 046(1)	0.417 0(8)	0.418 1(7) [27]	4
			0.416 5(9) [33]	
Dual Penrose tiling	0.465 145(1)*	0.465 2(8)		4
Ammann–Beenker tiling	0.418 878 00(1)	0.419 1(7)	0.418 6(7) [21]	4
Dual Ammann–Beenker	0.463 189 74(1)*	0.463 4(10)		4
Tübingen triangle tiling		0.256 5(6)		6
Square–triangle tiling		0.336 4(5)		$5.072\ldots \simeq 12 - 4\sqrt{3}$ [11]

the agreement of our data with the high-precision values [31] is even better than that of the other Monte Carlo values [21, 27, 33]. This is especially remarkable if one takes into account the small computational effort.

One can conclude from this that the values of the critical temperature for the 12-fold symmetric square–triangle tiling [5] and the 10-fold symmetric Tübingen triangle tiling [6] given in table 1 should have a similar accuracy. Also, they are in the correct rough range that one expects from the comparison of their first mean coordination number with those of the square and triangular lattice, see table 1.

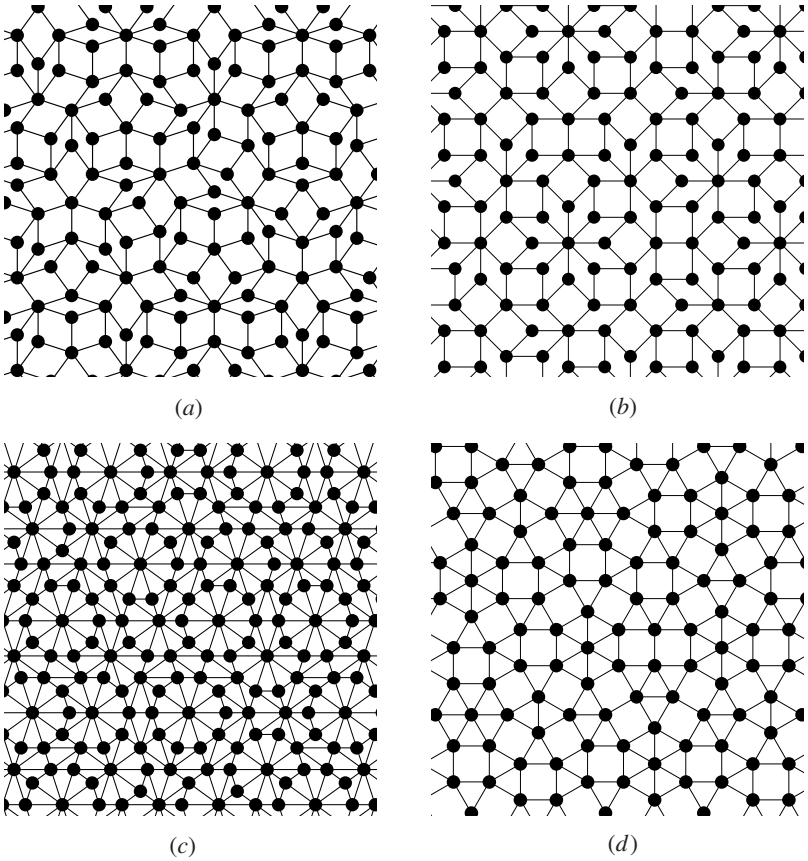

Figure 2. Parts of the quasiperiodic tilings considered here: (*a*) Penrose, (*b*) Ammann–Beenker, (*c*) Tübingen triangle and (*d*) 12-fold square–triangle tiling.

The autocorrelation times found were all compatible with those given in table 2 of [26], especially in the fact that they were always less than unity. Therefore, it seems safe to conclude that the IC algorithm is not significantly slower on quasiperiodic graphs than on periodic ones. In particular, it should still be much faster in finding the critical temperature (to the above-mentioned accuracy) than other Monte Carlo algorithms.

3. Generalization of the IC algorithm to non-identical coupling strengths

The IC algorithm has so far only been published for identical coupling strengths $J_{ij} \equiv J$, but a generalization to arbitrary ones is rather straightforward [23]. To this end, let us review how the Swendsen–Wang (SW) and IC algorithms are connected. In the SW algorithm, for each satisfied bond $\langle i, j \rangle$, a random number $0 \leqslant t_{ij} < 1$ is drawn from a uniform distribution and the bond is selected if the condition

$$t_{ij} < p_{ij} := 1 - \mathrm{e}^{-2\beta J_{ij}} \tag{3}$$

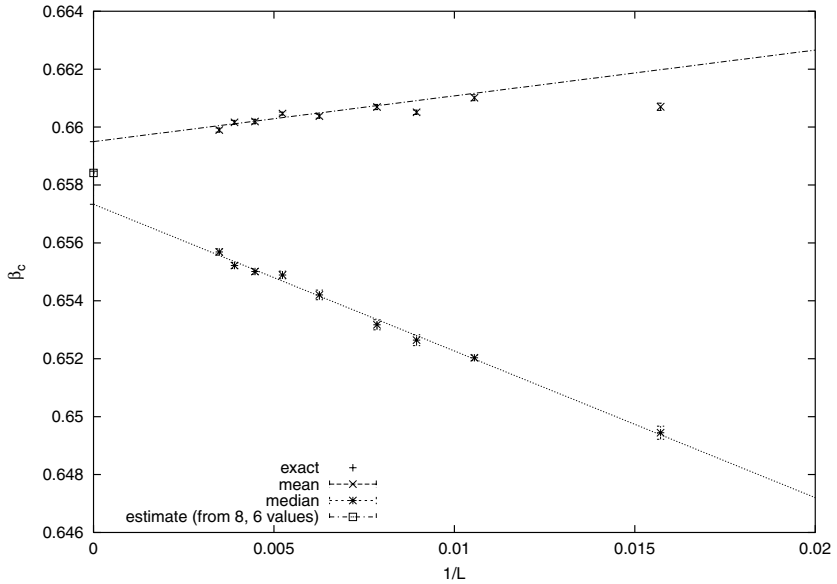

Figure 3. Finite-size scaling of the IC estimates of the inverse critical temperature on the hexagon packing.

is fulfilled. In the IC algorithm, by contrast, bonds are selected in random order until one cluster wraps around the system (or a different condition is met, see [12,25]). After solving (3) for β,

$$\beta < -\frac{1}{2J_{ij}} \log(1 - t_{ij}) =: \beta_{ij} \tag{4}$$

we see how the algorithm has to be generalized. We again draw a random number t_{ij} for each bond and calculate the corresponding β_{ij} from (4). Then we sort the bonds ascendingly with regard to β_{ij} and select the satisfied ones in this order until one cluster wraps around the system (or all satisfied bonds have been selected). If bond $\langle k, l \rangle$ was selected last, β_{kl} gives an estimate β_{est} for the inverse critical temperature.

The random numbers t_{ij} play a twofold role here. They determine the order in which the bonds are selected, and the one corresponding to the last bond selected gives the numerical value of β_{est}. So it is not necessary to use independent distributions for the t_{ij} as long as the marginal distributions are the same for all of them. Instead, one can use a random permutation of equidistant points 'approximating' the interval $[0, 1[$ for the t_{ij}. With such a choice, the original algorithm is recovered for identical couplings (in which case the sorting is trivial).

Now, there is a crucial difference between the original and the generalized version with regard to the computational complexity. In the case of identical couplings, only a permutation of the N bonds has to be created. This can be done with a computational effort of order $\mathrm{O}(N)$. The sorting of the arbitrary numbers β_{ij}, in contrast, requires an effort of $\mathrm{O}(N \log N)$ which makes the algorithm considerably slower. If, however, only a small (constant) number k of different coupling strengths is present, the sorting can be done with effort $\mathrm{O}(kN) = \mathrm{O}(N)$ by the following steps. (Let us assume all bonds to be numbered sequentially $1, \ldots, N$ here.)

1. Create an auxiliary permutation π of the numbers $\{1, \ldots, N\}$.

2. For each bond, define a value of the inverse temperature,

$$\beta_{\pi(i)} := -\frac{1}{2J_{\pi(i)}} \log\left(1 - \frac{2i-1}{2N}\right) \qquad i = 1, \ldots, N.$$

3. Create the final permutation Π of $\{1, \ldots, N\}$ by repeating the following steps for $i = 1, \ldots, N$ after initializing a list $(k_t)_{1 \leqslant t \leqslant k}$ with the indices of the first bonds of type t appearing in π.
   (a) Determine the value of t for which $\beta_{\pi(k_t)}$ becomes minimal.
   (b) Set $\Pi(i) := \pi(k_t)$.
   (c) Replace k_t by the next bond of type t appearing in π.

Steps 1 and 2 are possible with effort $O(N)$. In step 3, each of the k counters k_t takes on all the values $\{1, \ldots, N\}$ in the worst case. This step can therefore also be performed with effort $O(kN) = O(N)$. Overall, the sorting procedure takes linear computational effort, only with a higher constant than in the original algorithm.

The generalized IC algorithm will be applied to a class of Ising models with non-identical coupling strengths in the following section.

4. The Labyrinth tiling as an example to study the relevance of disorder

4.1. The Ising model on the Labyrinth tiling

The Labyrinth tiling [32] is constructed from a substitution ρ on the two-letter alphabet $\mathcal{A} = \{a, b\}$. Here we will consider substitutions of the type

$$\rho : \begin{array}{ccc} a & \to & b \\ b & \to & ba^k b \end{array}$$

with $k \geqslant 1$. The substitution is iterated infinitely, starting from the word b (or any other finite word), i.e. in each step it is applied to each letter of the word. This yields a (semi-)infinite limiting word w. For $k = 1$, we have the silver mean chain treated in [3]. Each letter is assigned an interval of a specific length. In this representation, the Cartesian product of w with itself is taken giving one quadrant of a (distorted) square lattice. Of this, one takes every other vertex, starting from the origin, and connects each one with its nearest neighbours over the diagonals of the underlying cells. As there are four types of those cells according to the letters $x, y \in \mathcal{A}$ on the vertical and horizontal copy of w, and each bond can be either 'raising' or 'lowering', we can distinguish 8 different types of bonds in the corresponding Ising model. We will denote the corresponding coupling strengths by J_{xy} for the raising and $\tilde{J}_{xy}$ for the lowering bonds. Part of the Labyrinth tiling corresponding to $k = 1$ is shown in figure 4.

On a four-dimensional submanifold of the eight-dimensional coupling space, the Ising model is exactly solvable and shows critical behaviour of Onsager type regardless of the underlying word w [3]. To see what the Harris–Luck criterion [16, 22] predicts, we have to look at the fluctuation exponent ω, which describes how the deviations of the mean coupling strength in a finite patch, compared with the infinite volume mean, scale with the size of the patch. If ω is greater than the 'critical' value $\omega_c = 1 - \frac{1}{d_m \nu}$ [22], one expects the disorder to be *relevant*, i.e. critical exponents deviating from the Onsager values. Here, ν is the correlation length exponent of the periodic system ($\nu = 1$ in our case) and the disorder affects all $d_m = 2$ dimensions, thus $\omega_c = \frac{1}{2}$. For $\omega < \omega_c$, the disorder is expected to be *irrelevant*. In the case of *marginal* disorder, $\omega = \omega_c$, the criterion does not make any specific predictions.

For substitution systems, the fluctuation exponent ω can be extracted from the bond substitution, which is in our case induced by the letter substitution ρ. It is given by

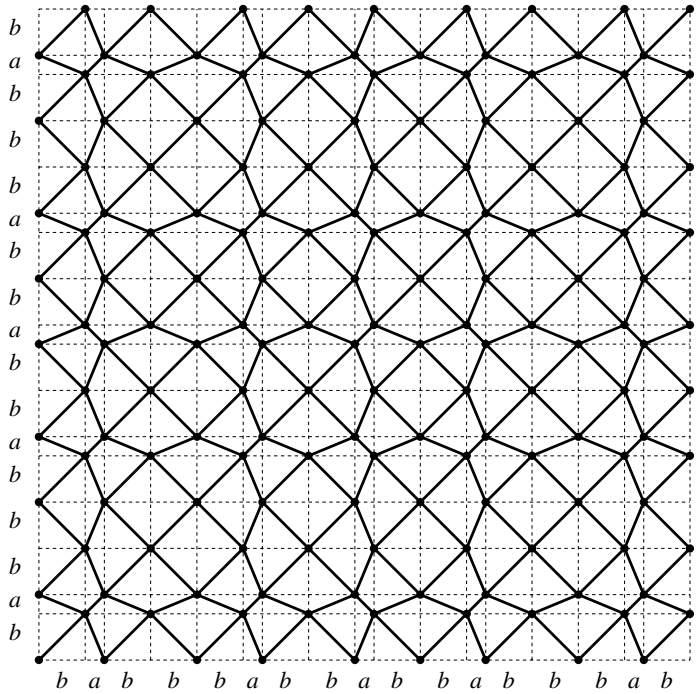

Figure 4. Part of the Labyrinth tiling corresponding to the substitution with $k = 1$.

$\omega = \log|\lambda_2|/\log\lambda_1$, where $\lambda_1 > |\lambda_2|$ are the two largest eigenvalues of the corresponding substitution matrix whose entries count how many bonds of one type (determined by the row of the matrix) are in the substitute for another type (the column). This matrix turns out to be described by the tensor product of the substitution matrix $M_\rho = \begin{pmatrix} 0 & k \\ 1 & 2 \end{pmatrix}$ for ρ with itself, its spectrum being $\sigma(M_\rho \otimes M_\rho) = \{\lambda\mu : \lambda, \mu \in \sigma(M_\rho)\}$ with $\sigma(M_\rho) = \{1 \pm \sqrt{1+k}\}$. Thus, we find the fluctuation exponent

$$\omega = \frac{\log k}{2\log(1+\sqrt{1+k})}. \tag{5}$$

Substitutions with $k < 3$ correspond to irrelevant disorder, $k = 3$ is the marginal case, and for $k > 3$ the disorder should be relevant. These predictions shall be tested shortly.

As an alternative model, let us also look at a random case. Instead of using a substitution for creating the word w, one can also use a random word of which each letter is independently chosen to be a or b with probability p_a and $(1-p_a)$, respectively. Due to the way the Labyrinth is constructed, the resulting bond distribution has correlations within each row and column. Accordingly, this kind of disorder has a higher fluctuation exponent than uncorrelated disorder, $\omega = \frac{3}{4}$ compared with $\omega = \frac{1}{2}$, and is relevant with respect to the Harris–Luck criterion.

4.2. Results

First, we successfully tested the implementation of the generalized algorithm on graphs with identical couplings and a few of the exactly solvable cases of the Labyrinth tiling.

Then, we applied the IC algorithm to the Ising model on the Labyrinth corresponding

Table 2. Choices for the coupling strengths used in the simulations for the Labyrinth tiling. Those for the raising and lowering bonds are denoted by J_{xy} and $\tilde{J}_{xy}$, respectively, where x and y are the corresponding letters in the horizontal and vertical copy of the word w.

Choice	J_{aa}	J_{ab}	J_{ba}	J_{bb}	$\tilde{J}_{aa}$	$\tilde{J}_{ab}$	$\tilde{J}_{ba}$	$\tilde{J}_{bb}$
#1	1.612 68	1	0.636 930 35	0.356 757 43	0.558 767 24	1	1.470 7784	2.108 427 2
#2	1.340 3778	1	0.773 081 47	0.550 515 91	0.719 494 98	1	1.264 4651	1.628 905 5
#3	0.4	0.8	1	2.8	1.980 992 8	1.228 5752	1	0.192 815 31
#4	2.5	1	0.5	0.75	0.251 595 91	1	1.734 3053	1.296 403 5
#5	1.2	1	0.7	2	1.4	0.9	1.1	1.8
#6	2.5	1	0.4	0.8	2.8	0.9	1.3	0.7
#7	0.4	0.8	1	2.8	1.3	2.3	0.9	2.4
#8	2	1.2	1.2	0.5	2	1.2	1.2	0.5

to the substitutions $k = 2, 3, 4$ and on the random version with $p_a = 0.4$, using the choices for the coupling strengths given in table 2. The first two choices (#1, #2) are on the exactly solvable submanifold, i.e. we chose three of the coupling strengths (J_{aa}, J_{ab}, J_{ba}) arbitrarily and the inverse critical temperature to be the one of the square lattice Ising model, $\beta_c = \operatorname{arsinh}(1)/2 \simeq 0.440\,69$, and determined the other five couplings by numerically solving the five equations [3]

$$\sinh(2\beta_c J_{xy}) \sinh(2\beta_c \tilde{J}_{xy}) = 1 \qquad x, y \in \mathcal{A} \tag{6}$$

and

$$\left(\frac{\sinh(2\beta_c J_{aa}) \sinh(2\beta_c J_{bb})}{\sinh(2\beta_c J_{ab}) \sinh(2\beta_c J_{ba})}\right)^2 \frac{\cosh(\beta_c[-\tilde{J}_{aa} + J_{ba} + \tilde{J}_{bb} + J_{ab}])}{\cosh(\beta_c[-J_{aa} + \tilde{J}_{ba} + J_{bb} + \tilde{J}_{ab}])}$$
$$\times \frac{\cosh(\beta_c[J_{aa} - \tilde{J}_{ba} + J_{bb} + \tilde{J}_{ab}]) \cosh(\beta_c[\tilde{J}_{aa} + J_{ba} - \tilde{J}_{bb} + J_{ab}])}{\cosh(\beta_c[\tilde{J}_{aa} - J_{ba} + \tilde{J}_{bb} + J_{ab}]) \cosh(\beta_c[J_{aa} + \tilde{J}_{ba} - J_{bb} + \tilde{J}_{ab}])}$$
$$\times \frac{\cosh(\beta_c[J_{aa} + \tilde{J}_{ba} + J_{bb} - \tilde{J}_{ab}])}{\cosh(\beta_c[\tilde{J}_{aa} + J_{ba} + \tilde{J}_{bb} - J_{ab}])} = 1. \tag{7}$$

The first four (6) are just the duality conditions on the lowering and raising bonds of the same type. The fifth one (7) involves all the remaining four coupling strengths. The next two choices (#3, #4) are self-dual but not exactly solvable, i.e. they fulfil the duality conditions (6) with respect to our chosen temperature, but the fifth condition (7) is significantly violated. The last four choices (#5 to #8) violate all five conditions. Choice #8 is isotropic, i.e. bonds are only distinguished with regard to their length.

We estimated the magnetic critical exponent $y_h = 2 - \beta/\nu$ as described in [12] by plotting the logarithm of the expectation value of the mass M of the cluster that wrapped around the system against the logarithm of the linear system size L and then taking a linear fit. As the expectation values of M and the magnetization of the system are the same, the usual scaling relation for the magnetization becomes $M \propto L^{y_h}$. Two examples are shown in figure 5; the results are summarized in table 3. For the exactly solvable choices (#1, #2), we always found the exponent to be of Onsager type and the critical temperature to agree with the exact solution, i.e. with the choice made above. For the self-dual choices (#3, #4), again, the Onsager exponent was found in all cases. The critical temperature, however, was not the chosen one for even values of k (2, 4), but agreed with it for odd ones (1, 3, 5) and probably also in the random version. (For the latter, the fluctuations in β_{est} were too large to state this unambiguously.) This is not yet understood.

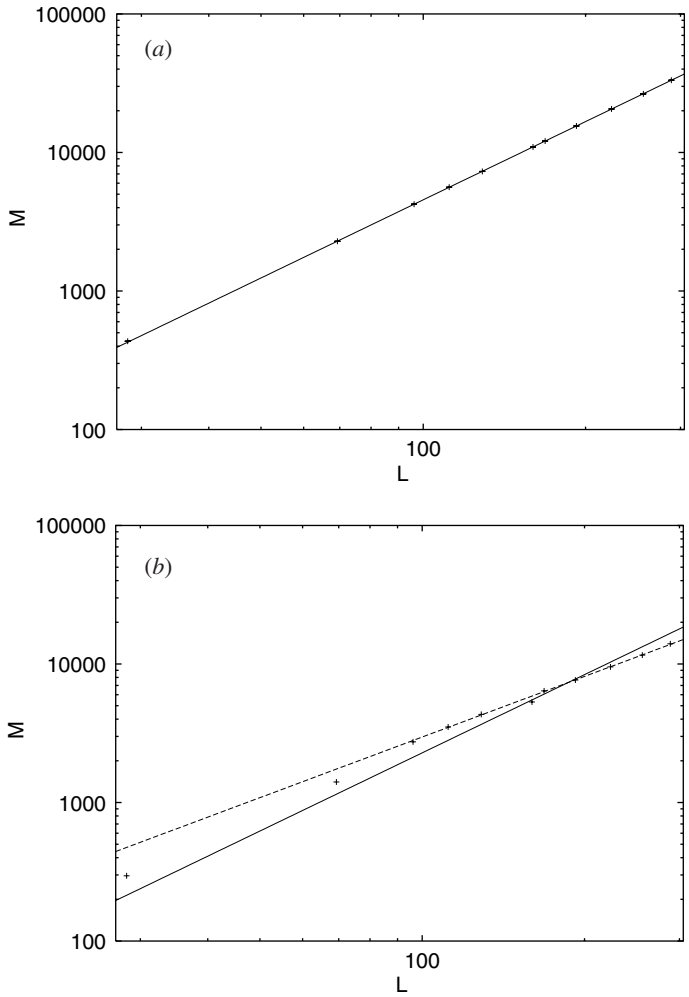

Figure 5. Determination of the magnetic exponent y_h on the Labyrinth tiling. The mass M of the cluster wrapping around the system is plotted versus the linear system size L. (*a*) is a typical example of Onsager behaviour (coupling choice #4 with $k = 4$) and (*b*) is typical of non-Onsager behaviour (choice #7 with $k = 4$). The solid lines have the Onsager slope $y_h = 1.875$, the dashed line is a linear fit yielding $y_h \simeq 1.453$. The fluctuations in (*b*) are due to variations in the bond frequencies in the approximants used.

For the arbitrary choices (#5 to #8), the critical exponent was of the Onsager class for $k = 2$. For $k \geqslant 3$, we still found power-law behaviour for all choices, but a significantly different exponent for choice #7 with $k = 4$. For the values in table 3 marked with †, no unique conclusion could be drawn, although the linear fits indicate deviations. With the clear deviation for choice #7, $k = 4$, and the predicition of the Harris–Luck criterion in mind, also choice #7 with $k = 3$ might be interpreted as a deviation from the Onsager value. Choice #5 and choice #8 with $k = 2$ are definitely compatible with the Onsager exponent, but the deviations might just be too small to be detected. In the random case, the fluctuations in M were too large to even confirm a power-law behaviour. This is probably due to the random fluctuations of the bond frequencies in the approximants used. For choices #1 to #4, however, the picture was qualitatively the same as in part (*a*) of figure 5.

Table 3. IC estimates of the magnetic critical exponent y_h on the Labyrinth tiling for three different substitutions and the random case, each one with the eight choices of the coupling strengths given in table 2. The value marked with * is significantly different from the Onsager value $y_h = 1.875$. Due to fluctuations as visible in part (*b*) of figure 5, the total error for the values marked with * or † is presumably quite large ($\approx$0.03). In the random case, the flucuations for choices #5 to #8 were too large to even confirm a power-law behaviour. The fluctuation exponent ω for the substitutions was computed using (5).

		Choice of couplings							
k	ω	#1	#2	#3	#4	#5	#6	#7	#8
2	0.345...	1.872	1.871	1.875	1.876	1.875	1.871	1.859	1.872
3	$\frac{1}{2}$	1.874	1.875	1.873	1.876	1.871	1.847†	1.732†	1.880
4	0.590...	1.872	1.873	1.877	1.875	1.866	1.839†	1.453*	1.898†
Random	$\frac{3}{4}$	1.874	1.878	1.877	1.862	fluctuations too large			

5. Summary and discussion

We tested the IC algorithm for the Ising model on various periodic and aperiodic planar graphs. A procedure was described that makes use of special properties of the algorithm in two dimensions and allows determination of the critical temperature with an accuracy of more than three significant digits. The computational effort for this is small compared with other Monte Carlo methods. Then we estimated the critical temperature on the 12-fold symmetric square–triangle tiling and the 10-fold symmetric Tübingen triangle tiling, two cases for which no values were known before. The values found are located in the rough range that one expects from the first mean coordination number of the tilings.

In the second part of the paper, we presented a generalized version of the algorithm applicable to models with non-identical coupling strengths. We applied it to the Ising model on the Labyrinth tiling for three different underlying substitutions, corresponding to irrelevant, marginal, and relevant disorder according to the Harris–Luck criterion, and a random case with relevant disorder. Each one was simulated for a few typical choices of the coupling strengths on the exactly solvable submanifold, on the self-dual but not exactly solvable submanifold, and away from both. The magnetic critical exponent $y_h = 2 - \beta/\nu$ was determined in all cases. The values found were compatible with the Onsager value for all self-dual subcases including the exactly solvable ones. For the latter this was known to be true exactly [3]. But it seems to extend to all self-dual cases even when the Harris–Luck criterion predicts deviations. For some (but not all) other choices of the coupling strengths, when the disorder was marginal or relevant according to the criterion, power-law behaviour with different exponents was observed in the substitution systems. The criterion can therefore be expected to be *generically* correct, but it does *not* exclude exceptions on lower-dimensional coupling manifolds. The sharp contrast seen in the random version between self-dual and not self-dual cases with respect to the absence, respectively presence, of large fluctuations of the mass of the cluster that wraps around the system might indicate that exceptions to the criterion are restricted to the self-dual submanifold. But further investigations are necessary to confirm this observation.

The IC algorithm has proved a good tool for efficiently obtaining quite accurate estimates of the critical temperature for periodic and aperiodic planar graphs. Although only one of the two independent critical exponents, the magnetic one, can be measured, this gives at least the possibility of detecting deviations from the Onsager universality class. Fortunately, it is a more sensitive quantity for this purpose than the specific heat exponent α, which is expected to remain zero when the disorder is increased [13].

Acknowledgments

OR is indebted to Jon Machta for introducing him to the field of cluster Monte Carlo algorithms during a nine-month stay in Amherst in 1996/7 and for important discussions during this work. We thank Uwe Grimm and Joachim Hermisson for stimulating discussions. Useful hints by the referees are gratefully acknowledged. Financial support was given by the German Research Council (DFG).

References

[1] Ammann R, Grünbaum B and Shephard G 1992 Aperiodic tiles *Discrete Comput. Geom.* **8** 1–25
[2] Baake M 2001 A guide to mathematical quasicrystals *Quasicrystals* ed J-B Suck, M Schreiber and P Häußler (Berlin: Springer) to be published
(Baake M 1999 *Preprint* math-ph/9901014)
[3] Baake M, Grimm U and Baxter R J 1994 A critical Ising model on the Labyrinth *Int. J. Mod. Phys.* B **8** 3579–600
[4] Baake M, Grimm U, Repetowicz P and Joseph D 1998 Coordination sequences and critical points *Proc. Int. Conf. on Quasicrystals (Tokyo)* vol 6, ed S Takeuchi and T Fujiwara (Singapore: World Scientific) pp 124–7
(Baake M, Grimm U, Repetowicz P and Joseph D 1998 *Preprint* cond-mat/9809110)
[5] Baake M, Klitzing R and Schlottmann M 1992 Fractally shaped acceptance domains of quasiperiodic square-triangle tilings with dodecagonal symmetry *Physica* A **191** 554–8
[6] Baake M, Kramer P, Schlottmann M and Zeidler D 1990 Planar patterns with fivefold symmetry as sections of periodic structures in 4-space *Int. J. Mod. Phys.* B **4** 2217–68
[7] Barber M N 1983 Finite-size scaling *Phase Transitions and Critical Phenomena* vol 8, ed C Domb and J L Lebowitz (London: Academic) pp 146–266
[8] Beenker F P M 1982 Algebraic theory of non-periodic tilings of the plane by two simple building blocks: a square and a rhombus *Techn. Univ. Eindhoven TH-Report* 82-WSK-04
[9] Bhattacharjee S M, Ho J-S and Johnson J A Y 1987 Translational invariance in critical phenomena: Ising model on a quasi-lattice *J. Phys. A: Math. Gen.* **20** 4439–48
[10] Binder K 1981 Finite size scaling analysis of Ising model block distribution functions *Z. Phys.* B **43** 119–40
[11] Briggs K 1993 Self-avoiding walks on quasilattices *Int. J. Mod. Phys.* B **7** 1569–75
[12] Choi Y S, Machta J, Tamayo P and Chayes L X 1999 Parallel invaded cluster algorithm for the Ising model *Int. J. Mod. Phys.* C **10** 1–16
[13] Dotsenko V 1995 Critical phenomena and quenched disorder *Phys. Usp.* **38** 457–96
(Dotsenko V 1995 *Usp. Fiz. Nauk.* **165** 287–96 (in Russian))
[14] Franzese G, Cataudella V and Coniglio A 1998 Invaded cluster dynamics for frustrated models *Phys. Rev.* E **57** 88–93
[15] Grimm U and Baake M 1997 Aperiodic Ising models *The Mathematics of Long-Range Aperiodic Order* ed R V Moody (Dordrecht: Kluwer) pp 199–237
[16] Harris A 1974 Effect of random defects on the critical behaviour of Ising models *J. Phys. C: Solid State Phys.* **7** 1671–92
[17] Hermisson J 2000 Aperiodic and correlated disorder in XY-chains: exact results *J. Phys. A: Math. Gen.* **33** 57–69
[18] Hermisson J 1999 Aperiodische Ordnung und magnetische Phasenübergänge *PhD Thesis* (Aachen: Shaker-Verlag)
[19] Hermisson J 1999 Renormalization of two-dimensional Ising systems with irrelevant, marginal and relevant aperiodic (dis)order *Mat. Sci. Eng.* A at press
[20] Hermisson J, Grimm U and Baake M 1997 Aperiodic Ising quantum chains *J. Phys. A: Math. Gen.* **30** 7315–35
[21] Ledue D, Landau D P and Teillet J 1995 Static critical behaviour of the ferromagnetic Ising model on the quasiperiodic octagonal tiling *Phys. Rev.* B **51** 15 523–30
[22] Luck J M 1993 A classification of critical phenomena on quasi-crystals and other aperiodic structures *Europhys. Lett.* 359–64
[23] Machta J 1998 Private communication
[24] Machta J, Choi Y S, Lucke A, Schweizer T and Chayes L M 1995 Invaded cluster algorithm for equilibrium critical points *Phys. Rev. Lett.* **75** 2792–5
[25] Machta J, Choi Y S, Lucke A, Schweizer T and Chayes L M 1996 Invaded cluster algorithm for Potts models *Phys. Rev.* E **54** 1332–45

[26] Moriarty K, Machta J and Chayes L Y 1999 Dynamic and static properties of the invaded cluster algorithm *Phys. Rev.* E **59** 1425–34
[27] Okabe Y and Niizeki K 1988 Monte Carlo simulation of the Ising model on the Penrose lattice *J. Phys. Soc. Japan* **57** 16–9
[28] Penrose R 1974 The rôle of aesthetics in pure and applied mathematical research *Bull. Int. Math. Appl.* **10** 266–71
[29] Redner O 1999 Effiziente Simulation periodischer und nicht-periodischer Ising-Modelle am kritischen Punkt *Diploma Thesis* University of Tübingen (available from the author)
[30] Repetowicz P, Grimm U and Schreiber M 1999 High-temperature expansion for Ising models on quasiperiodic tilings *J. Phys. A: Math. Gen.* **32** 4397–418
[31] Repetowicz P, Grimm U and Schreiber M 1999 Planar quasiperiodic Ising models *Mat. Sci. Eng.* A at press (Repetowicz P, Grimm U and Schreiber M 1999 *Preprint* cond-mat/9908088)
[32] Sire C, Mosseri R and Sadoc J-F 1989 Geometric study of a 2D tiling related to the octagonal quasiperiodic tiling *J. Physique* **50** 3463–76
[33] Sørensen E S, Jarić M V and Ronchetti M 1991 Ising model on Penrose lattices: boundary conditions *Phys. Rev.* B **44** 9271–82
[34] Swendsen R H and Wang J-S 1987 Nonuniversal critical dynamics in Monte Carlo simulations *Phys. Rev. Lett.* **58** 86–8
[35] Syozi I 1972 Transformation of Ising models *Phase Transitions and Critical Phenomena* vol 1, ed C Domb and M S Green (London: Academic) pp 269–329
[36] Wolff U 1989 Collective Monte Carlo updating for spin systems *Phys. Rev. Lett.* **62** 361–4